Journal of Materials Chemistry B

Accepted Manuscript

ROYAL SOCIETY OF CHEMISTRY

www.rsc.org/materialsB

Research Papers

Running header: preferential uptake of brick shaped nanoparticles in endothelium.

Differential Internalization of Brick Shaped Iron Oxide Nanoparticles by Endothelial Cells

Zhizhi Sun[1], Matthew Worden[2], Yaroslav Wroczynskyj[3], Palash K. Manna[3], James A. Thliveris[4], Johan van Lierop[3], Torsten Hegmann[1,2,5], Donald W. Miller[1].

[1]Department of Pharmacology and Therapeutics, University of Manitoba, Winnipeg, Manitoba, Canada

[2]Department of Chemistry and Biochemistry, Kent State University, Kent, OH, U.S.A.

[3]Department of Physics and Astronomy, University of Manitoba, Winnipeg, Manitoba, Canada

[4]Department of Human Anatomy and Cell Sciences, University of Manitoba, Winnipeg, Manitoba, Canada

[5]Chemical Physics Interdisciplinary Program, Liquid Crystal Institute, Kent State University, Kent, OH, U.S.A.

Correspondence: Donald W. Miller

Department of Pharmacology and Therapeutics, 710 William Avenue, University of Manitoba, Winnipeg, Manitoba, Canada. R3E 0T6

Tel +1 204 789 3278

Fax +1 204 789 3932

Email donald.miller@umanitoba.ca

Abstract

Nanoparticles targeting endothelial cells to treat diseases such as cancer, oxidative stress, and inflammation have traditionally relied on ligand-receptor based delivery. The present studies examined the influence of nanoparticle shape in regulating preferential uptake of nanoparticles in endothelial cells. Spherical and brick shaped iron oxide nanoparticles (IONPs) were synthesized with identical negatively charged surface coating. The nanobricks showed a significantly greater uptake profile in endothelial cells compared to nanospheres. Application of an external magnetic field significantly enhanced the uptake of nanobricks but not nanospheres. Transmission electron microscopy revealed differential internalization of nanobricks in endothelial cells compared to epithelial cells. Given the reduced uptake of nanobricks in endothelial cells treated with caveolin inhibitors, the increased expression of caveolin-1 in endothelial cells compared to epithelial cells, and the ability of IONP nanobricks to interfere with caveolae-mediated endocytosis process, a caveolae-mediated pathway is proposed as the mechanism for differential internalization of nanobricks in endothelial cells.

Keywords: shape, iron oxide nanoparticles, drug delivery, nanobrick, endothelial cells, endocytosis, caveolae

Background

There is a growing interest in developing iron oxide nanoparticles (IONPs) as platforms for drug delivery applications.[1-3] In this regard, IONPs provide several advantages: 1) The ability to target to areas of interest using externally applied magnetic field, thereby increasing local therapeutic concentrations of IONPs and decreasing potential toxicity related to systemic circulation. 2) Monitoring capabilities for IONPs using MRI. 3) Favorable biocompatibility profile. 4) Flexibility of surface modification to create multifunctional complexes for advanced drug delivery applications involving intracellular or plasma membrane targets. The interaction between IONPs and the cell membrane is largely determined by their physiochemical properties such as surface coating and shape.[4, 5] Our group has previously examined the effect of surface charge on the cellular uptake of IONPs.[6] We found that positively charged IONPs have a significantly higher uptake profile compared to negatively charged ones, likely due to electrostatic interactions between positively charged IONPs and the negatively charged plasma membrane of the cell. As a result, negatively charged nanoparticles appeared to be better candidates to advance in our drug delivery platform due to the potential for longer circulation times and reduced clearance. However, the charge related effects on internalization were non-specific as they were present in a variety of different cell types.[6]

Various pathological conditions such as cancer, cardiovascular disease, inflammation, and oxidative stress would benefit from the preferential delivery of nanoparticles to the vascular endothelium.[7-9] To achieve the cell specific delivery, targeting ligands are often grafted onto the NPs to increase the delivery efficiency. For instance, intracellular adhesion molecule (ICAM), vascular cell adhesion molecule (VCAM), and platelet-endothelial cell adhesion molecule (PECAM-1) have been used to target endothelial cells.[10-12] However, these approaches are often associated with variability in outcome due to different receptor expression levels between patients or heterogeneity of endothelial cells within different

tissue.[13] Therefore, a generalized approach that preferentially target endothelial cells without ligand receptor interaction would be advantageous.

In addition to surface charge, nanoparticle shape may also play a role in cell interactions. To date, there are few reports concerning non-spherical nanoparticles. Recent work with theoretical modeling revealed the role of nanoparticle shape and membrane rigidity on cellular uptake.[14] However, only a handful of studies provide side-by-side comparison of spherical and non-spherical nanoparticle interactions with biological environments. [15] Recent advances in synthesis techniques have enabled creation of brick shaped IONPs.[16] We hypothesize that changing the IONP shape will influence both the cellular uptake in endothelial cells and the ability to augment cell uptake with application of an external magnetic field. Toward that end, the uptake profiles of iron oxide nanospheres and nanobricks of similar size in various cell types were examined to address the impact of IONP shape. In addition, the mechanism of preferential uptake of the nanobrick IONPs in endothelial cells was determined with evidence suggesting a caveolin-dependent process. By understanding the relationship between IONP shape and cell surface domains, our work provides insight into the development of IONPs for specifically targeting endothelial cells.

Methods

Materials

All chemical reagents were purchased from Sigma Aldrich (St. Louis, MO) and cell culture reagents from Invitrogen Canada Inc. (Burlington, ON) unless otherwise specified.

Nanoparticle synthesis and characterization

Sphere shaped iron oxide nanoparticles were prepared under mild conditions at room temperature as previously described.[17] They were prepared by adding N-(trimethoxysilylpropyl)ethylenediaminetriacetate trisodium salt (EDT, 3 mmol, from a solution concentration of 45% in water) (Gelest, Morrisville, PA) directly to a reaction vessel containing IONPs . The mixture was allowed to react overnight with stirring and the final product was purified by dialysis (MWCO 30000) against deionized (DI) water over 48 hours and was freeze dried and resuspended in sterile PBS prior to experiments. Brick shaped IONPs with EDT surface coating was synthesized and prepared as recently described.[16]

Nanoparticle crystallographic properties of both the nanospheres and nanobricks were measured with powder x-ray diffraction experiments using a Brüker diffractometer (D8 Discover with Davinci; Karlsruhe, Germany). Both nanoparticle systems were identified as iron oxide through Reitveld refinement incorporating the effects of the nanocrystalline nature of the samples (e.g. Scherrer broadening effects).

The IONP size distribution in DI water was determined initially through photon correlation spectroscopy (PCS) at a fixed scattering angle (90°) using a Horiba Nano-Partica SZ-100 series instrument (Horiba Instruments Inc., Irvine, CA). The same instrument allowed for the assessment of particle surface charge (zeta potential) by the measurement of IONP electrophoretic mobilities using phase analysis light

scattering. The magnetization of dry nanoparticle powder samples were recorded at room temperature as a function of applied magnetic field (0 – 4 T) using a Quantum Design MPMS XL SQUID magnetometer (San Diego, CA).

Cell culture

A mouse brain derived microvessel endothelial cell line, bEnd.3 (American type tissue culture collection, Manassas, VA), was used as a cell culture model of the blood-brain barrier (BBB). The bEnd.3 cells (passage number 15-30) were cultured in DMEM (Hyclone, Logan, UT) supplemented with 10% heat-inactivated FBS (Hyclone, Logan, UT), 50 U/mL penicillin and streptomycin (MP Biomedicals, Solon, OH) at 37°C and 5% CO_2. Cells were expanded in T-75 tissue culture flasks, and seeded at $2x10^4$ cells per cm^2 on 6 or 12 well plates for uptake and cytotoxicity studies, respectively. Culture medium was changed every 2 days. All experiments were performed on confluent monolayers (typically 4-5 days post seeding).

Cellular Uptake of IONP compositions

Confluent monolayers of bEnd.3 cells grown on 6-well culture plates (Costar, Lowell, MA) were treated with culture media containing either nanosphere or nanobrick compositions (2.5μg/mL – 100μg/mL of Fe). After treatment with IONPs, cells were placed in a humidified CO_2 incubator maintained at 37°C. After 4 hours, the IONP solutions were removed and the cell monolayers were washed 3X with ice cold phosphate buffered saline (PBS) to remove unbound nanoparticles. Cells were lysed by the addition of 500 μl of 0.2 M NaOH and IONP content determined based on the ferrozine assay described below. Cellular accumulation was examined in both the presence and absence of a static magnetic field created by placing the cells over a platform containing cylindrical rare earth magnets (19mm diameter, 3mm height) (Lee Valley, Ottawa, ON, Canada). Cells remained in the magnetic field for the duration of the experiment.

For mechanistic studies of IONP uptake experiments were performed at both 4^{O} and 37^{O} C and in the presence of various endocytotic inhibitors. Cells were pretreated with chlorpromazine (7 μg/mL), methyl-beta-cyclodextrin (10mM), genistein (200μM), monensin (25μM), or cytochalasin D (5 μg/mL) for 30 min at 37°C. Cells were exposed to the nanobricks for 1 h at 37°C in the presence of the various endocytotic inhibitors. Cell association of nanobricks was determined as described below. Additional studies using known markers of caveolae mediated endocytosis, alexa fluor 488-labeled cholera toxin subunit B (CTB) and tetramethylrhodamine conjugated bovine serum albumin (BSA) were examined for cellular uptake. For these studies, cells were exposed to CTB (3.5 μg/mL), BSA (10 μg/mL) for 2 h either alone or following 15-min pretreatment with various concentrations of the iron-oxide nanobricks. Cells were washed and lysed and fluorescence determined using a Synergy HT plate reader (BioTek, Winooski, VT).

Analytical assay for measuring IONPs

Quantitative determination of IONP content in cell and media samples was performed using the Ferrozine assay. As the Ferrozine assay is an absorbance-based assay for determining soluble iron concentrations, IONPs in the cell lysate and media samples were first solubilized by adding 500 μL of concentrated HCl (~12M) to 500 μL of cell lysate or media samples. This mixture was incubated for 1 h at room temperature with gentle shaking and then neutralized with 500 μL of 12M NaOH. Once the samples were neutralized, 120 μL of hydroxylamine hydrochloride (2.8 M) in 4M HCl was added and the samples incubated for 60 min at room temperature with gentle shaking. Following this incubation, 50 uL of 10 M ammonium acetate solution (pH 9.5) and 300 uL of 10mM ferrozine in 0.1M ammonium acetate solution were added to each sample. Absorbance was measured at 562 nm using a Synergy HT plate reader (BioTek, Winooski, VT). Quantitative assessment of IONP concentration was based on a standard curve prepared by serial dilutions of 1000 ppm iron atomic absorption standard (Fisher Scientific, Ottawa, ON). Samples from the cell lysates were normalized for protein content using BCA protein assay kit (Pierce, Rockford, IL).

Electron Microscopy

The cellular localization of IONPs compositions was examined using transmission electron microscopy. For these studies, cells were incubated with IONPs at 50μg/mL concentration in media for 2 hours. After incubation, cells were washed 3X with PBS and collected using 0.25% trypsin EDTA (Hyclone, Logan, UT). After centrifugation, the cell pellets where fixed in 3% glutaraldehyde in 0.1M phosphate buffer (pH 7.3), followed by post-fixation in 1% osmium tetroxide in 0.1M phosphate buffer (pH 7.3). Cells were then dehydrated and embedded in Epon 812 using standard techniques.[18] Thin sections were stained with uranyl acetate and lead citrate, viewed and photographed in a Philips CM 10 electron microscope (FEI, Hillsboro, OR, USA). In order to eliminate observer bias, sections were examined without foreknowledge of their source.

Statistical analysis

All data were expressed as mean ± SEM. All values were obtained from at least three independent experiments. Statistical significance was evaluated using one-way ANOVA followed by post-hoc comparison of the means using the Tukey's test.

Results

Physico-chemical characterization of IONPs

Physico-chemical parameters of the nanobrick and nanosphere compositions are provided in Figure 1. Both nanobricks and nanospheres were silanized and had free carboxylic acid functional groups on their surfaces resulting in zeta potentials of approximately -40 mV. The TEM images confirming the different shapes of IONPs have previously been published.[16, 17] The dimensions of IONP core for the nanobricks were approximately 15 nm x 10 nm x 5nm while the nanosphere was around 8 nm in diameter. The saturation magnetization, determined by fitting the high field magnetization to a straight line after background subtraction (diamagnetic signal from the sample holder), was 50 ± 5 A m^2 kg^{-1} and 10 ± 2 A m^2 kg^{-1} for the nanobricks and nanospheres, respectively. The saturation magnetization is the largest magnetization that a material can exhibit in an applied magnetic field. Samples with larger saturation magnetizations have greater magnetic response and thus are likely more useful for targeted delivery using an externally applied magnetic field. A more detailed description of the nanoparticle's characterization is provided in the Supplementary Information.

Preferential internalization of nanobrick in endothelial cells

Quantitative uptake analysis was performed in the bEnd.3 mouse brain endothelial cell line. (Figure 2a) In absence of magnetic field, there was a significantly greater uptake of nanobrick compared to nanosphere compositions at all concentrations above 5μg/mL. In the presence of external magnetic field, cell association of nanobrick was substantially increased compared to nanosphere. At the highest concentration examined (100μg/mL), there was a 30-fold and 10-fold increase in uptake of nanobricks compared to nanospheres with and without a magnetic field, respectively. This surprising finding suggests that despite the negative surface charge, brick shaped IONPs are taken up by brain endothelial cells to a greater extent than spherical counterparts. Furthermore, the shape of IONPs affected their magnetization value and ability to interact with cells in the presence of an external magnetic field gradient. Potential

toxicity of nanobricks related to bEnd.3 cells was investigated (Figure S1). Nanobricks appear to be non-toxic even at 100 ug/mL concentration.

Uptake studies with the nanobrick was expanded to include primary human lung and brain endothelial cells as well as Madin-Darby canine kidney (MDCK) epithelial cell line with two fold purpose: 1) To investigate whether there was any selectivity to endothelial cells versus epithelial cells; and 2) To examine whether enhanced uptake of the nanobricks was specific to brain endothelial cells compared to other endothelial beds. External magnetic field significantly enhanced cellular uptake of nanobricks in both the lung and brain microvessel endothelial cells but not in epithelial cells (MDCK) (Figure 2b). While accumulation of the nanobrick IONPs in the presence of an external magnetic field was significantly greater in the endothelial cells compared to the epithelial cell line, there was no apparent differences between endothelial cells from different vascular beds (Figure 2b). Transmission electron microscopy (TEM) of the various cell preparations confirmed that nanospheres were loosely bound on the cell surface and not internalized by bEnd.3 cells (Figure 3a) or human hepatocellular liver carcinoma cell line HepG2 (Figure 3b). By contrast, large amounts of nanobricks were found inside the bEnd.3 endothelial cells (Figure 3c) but few were found inside HepG2 (Figure 3d) or MDCK epithelial cell lines (Figure 3e), confirming the finding that the nanobricks were selectively internalized in endothelial cells.

Internalization of nanobrick in bEnd.3 cells via caveolae mediated endocytosis

To understand the selectivity of nanobricks to endothelial cells, we examined the potential mechanism of internalization. The observation that nanobrick accumulation in bEnd.3 cells was temperature dependent with significantly less uptake at 4O compared to 37O C suggested an energy dependent endocytic process (Figure S2). To determine which type of process was responsible for uptake of the nanobricks, confluent bEnd.3 cell monolayers were pretreated with inhibitors for clathrin mediated endocytosis (chlorpromazine), caveolae mediated endocytosis (MβCD, genistein), macropinocytosis (cytochalasin D), and endosome maturation (monensin) for 30 min, and uptake of nanobricks at 100 ug/mL was determined

(Figure 4a). There was a significant inhibition of nanobrick uptake in the MβCD and genistein treatment groups (Figure 4a). These findings were confirmed in TEM studies showing diminished IONP association in bEnd3 in the presence of genistein compared to controls receiving the nanobricks alone (Figure 4b,c). The inhibition observed with genistein and MbCD was not attributable to toxicity based inhibition of uptake as none of the inhibitors examined showed cytotoxicity at the concentrations examined in bEnd.3 cells (Figure S3). None of the other treatment groups examined significantly impacted on nanobrick accumulation in bEnd3 cells (Figure 4a), suggesting that nanobrick internalization in bEnd.3 cells was mediated via a caveolae dependent endocytosis pathway.

To ascertain whether elevated caveolae mediated endocytosis in endothelial cells contributes to the selective internalization of nanobricks observed in endothelial cells, additional studies were performed with known markers of caveolae-mediated endocytosis. The uptake of CTB and BSA is 6-fold and 12-fold greater in bEnd.3 cells than MDCK cells, respectively. (Figure 5a) The increase in uptake of CTB and BSA in the bEnd3 was correlated with an increase in the expression of caveolin-1 compared to epithelial MDCK cell line. Expression of caveolin-1 in another endothelial cell line hCMEC/D3 was also elevated. (Data not shown) Additional evidence of potential interaction of nanobricks in caveolae-mediated endocytosis is the ability of the nanobricks to inhibit the uptake of fluorescently-labeled BSA in a concentration dependent manner. (Figure 5b)

Discussion

Previous studies by our laboratory and others[19-22] have demonstrated the importance of surface charge of IONPs for cellular uptake. In the present study, negatively charged IONPs of different shape were utilized to examine the influence of shape on cellular uptake. While there are some publications regarding the synthesis of different shaped IONPs,[23, 24] these methods are typically thermal decomposition based generating nanoparticles that are not directly dispersible in water and therefore not readily amenable to cell based interactions. With regards to the possible impact of IONP shape on cell uptake, to date the shape-dependent impact on the cell accumulation have been limited to macrophages, fibroblast, and cancer cells.[25-27] The current studies are the first to demonstrate a shape related effect on IONP accumulation in endothelial cells. Our results demonstrated that brick shaped IONPs were preferentially taken up by endothelial cells compared to sphere shaped IONP with identical surface coatings. In addition, when studies were performed in the presence of a magnetic field, the endothelial sensitivity for nanobrick accumulation was even more apparent, being substantially greater than epithelial cell preparations. The selective uptake of the nanobricks by endothelial cells appears to be due to caveolae-mediated endocytosis, which is more prevalent in endothelial cells compared to epithelial cells examined.

As the nanobricks are slightly larger than the nanospheres (15 x 10 x 5nm for nanobricks vs 8nm diameter nanospheres), there is a possibility that differences in size may also contribute to the increased accumulation of IONP nanobricks in the endothelial cells. Previous studies demonstrated a size dependent effect on IONP accumulation in the Caucasian colon adenocarcinoma cell line (Caco2).[28] However, it should be noted that those IONP had a positive surface charge and were considerably larger (30 - 100 nm core diameter) than the IONP used in the present study. Given the EDT surface coating used in the present study, the studies of Saito et al reporting no size dependent effect on the accumulation of negatively charged IONP in cells may be more relevant. In this study, the cellular uptake of alkali-treated dextran coated IONPs (-15mV zeta potential) with particle sizes of 28 and 74 nm, were compared to that

of carboxymethyl dextran IONPs (-24mV zeta potential) of similar size in a macrophage cell line, RAW264. While there was a clear surface charge dependency in cell accumulation, with the alkali-treated dextran coated IONPs having greater accumulation than the carboxymethyl dextran coated IONPs, no significant difference was found in the cellular accumulation of the large (74 nm diameter) and small (28 nm diameter) IONPs of the same coating.[29] Taken together, these studies would suggest that for the negatively charged particles with low membrane association, size is not the predominant factor for determining cellular accumulation.

We found that brick shaped IONPs could enhance the affinity between surface coating and cell membrane compositions. An increased contact area with the cell surface provides potentially more sites for interaction and has been previously identified as an important contributor to enhance nanoparticle targeting effects.[30] Our finding is in line with recent publications of shape related effect on polystyrene NPs. Barua et al reported that rod shaped polystyrene NPs have enhanced antibody binding specificity to three breast cancer cell lines compared to spherical and disk shaped NPs.[31] Using *in silico* and *in vivo* approaches, Kohlar and colleagues demonstrated rod shaped polystyrene NPs with antibody against intracellular adhesion molecule (ICAM) or transferrin receptor exhibited higher internalization in brain and lung endothelial cells than spherical counterparts under flow conditions.[32] Hence, it is speculated that by changing the IONPs from sphere to brick, the negatively charged surface coating interacts with multiple discrete sites on the cell membrane that contributes to the selective binding of the nanobricks to endothelial cells. This may provide advantages especially when second-generation nanobrick compositions are created that have additional endothelial ligand targeting capabilities. We further hypothesize that a low affinity ligand grafted on nanobrick surface would exhibit a stronger interaction to its receptor than grafted on nanospheres. Such studies are currently ongoing.

Generally speaking, physiochemical properties of IONPs such as shape and surface coating would be expected to have an impact on the internalization pathway. Studies by Hsu et al demonstrated that

chitosan coated IONPs and hyaluronan-modified chitosan coated IONPs may activate different endocytosis pathways. In these studies, chitosan coated IONPs favored uptake by clathrin mediated endocytosis, while the hyaluronan modified chitosan favored more caveolae mediated endocytosis routes.[33] Our previously published studies using positively charged amino silane coated and negatively charged amino silane with EDT functionalized end groups demonstrated that the negatively charged EDT coated nanospheres had a much lower cellular accumulation than the positive charged IONP. This observation, that negatively charged IONP had lower uptake than positively charged IONP of similar size and shape, held up across a variety of cells including brain endothelial cells, as well as primary cultured neurons and astrocytes.[6] This is due to the fact that negatively charged surface reduces nonspecific electrostatic interactions between the NPs and cell surface. The results of the present study, that the EDT coated nanobricks with identical surface coating and similar size as the nanospheres showed dramatic increases in uptake in endothelial cells, suggest that while the coating of the nanoparticle is important, so too is the shape. Furthermore at least for the EDT coated IONPs, shape appears to be a bigger determinant of caveolae-mediated vesicular transport.

Of the various vesicular internalization processes, caveolae mediated endocytosis is predominantly found in endothelial cells.[34] Therefore, targeting to endothelial cells may be achieved by interacting with caveolae localized in lipid rafts within the plasma membrane. The current study certainly points to a caveolae-mediated mechanism for the endothelial selective uptake of the nanobrick IONP. The evidence in support of this is the increased expression of caveolin in endothelial cells compared to the epithelial cells and the ability of inhibitors of caveolae-mediated uptake to significantly reduce nanobrick IONP accumulation in endothelial cells. In addition, the nanobrick IONPs were able to prevent the cellular uptake of two macromolecules, CTB and BSA, which are known to enter into endothelial cells through caveolae-mediated endocytosis in a concentration dependent manner consistent with competitive inhibition of caveolae biding sites. Previous studies grafting anionic polyelectrolytes of varied hydrophobicity to nanospheres reported endothelial cell targeting of NPs via a caveolae-mediated

endocytic process.[35] These findings together suggest that non-spherical nanoparticles with negative surface charges are likely to have the greatest affinity for caveolae-based uptake.

Caveolae are formed by a group of caveolin protein binding to cholesterol in the lipid raft region of the cell membrane.[36] Although surface chemistry and functional groups can influence IONP cell interaction, it has been reported that negatively charged IONPs can interact with cationic lipid domains in the lipid raft.[37] Caveolae are enriched in endothelial cells and present in muscle, fibroblast, and adipocytes.[38] Following the pinch off of caveolae from the lipid raft, the fate of caveolae is dependent on the cell type in which endocytosis occurs. In non-endothelial cells, caveolae are subjected to the endosomal-lysosomal system. In endothelial cells, caveolae may bypass the lysosome and transport cargo through vesicular processes across the endothelial cell layer.[39, 40] For this reason, the nanobrick IONPs may potentially be exploited for drug and gene delivery applications to tissues underlying endothelial cells such as the brain. These studies are currently ongoing.

Compared to nanospheres, the nanobricks have an increased responsiveness in an applied magnetic field gradient. Based on the modeling and simulation data, (the nanobricks have a preferred direction of magnetization along their largest dimension (see Figure S4) As such, an externally applied magnetic field will act to more preferentially to align the smaller dimensions of the nanobricks along the cell surface, decreasing the area of interaction and thus limiting the effect of the steric repulsion between the cell surface and nanobrick coating. The proposed behavior of the nanobricks in the externally applied magnetic field may help explain the significant increase in uptake of the nanobricks compared to the nanosphere observed in the presence of a magnetic gradient in the present study. In addition to the potential for tissue targeting using external magnetic fields, the magnetic properties of the nanobricks made them ideal candidates for magnet resonance imaging agents. Nanobricks show large and constant transverse relaxivity (r_2) for medium and high-field MRI compared to gadolinium based contrast agents that peaks at 20 MHz and decreases quickly with high magnetic fields.[16]

The preferential uptake of nanobrick IONPs within vascular endothelial cells combined with the enhanced targeting through application of external magnetic fields has several potential therapeutic applications. The ability to target to the endothelial cells within tumor microvasculature is a prime application for this technology platform. It is generally accepted that angiogenesis is crucial for tumor growth, evasion and metastasis.[41] The creation of new blood vessels to supply oxygen and nutrients to tumor cells is a necessary requirement for solid organ tumor growth. Thus, anti-angiogenesis therapy has emerged as a viable treatment strategy to control tumor growth. Recent studies demonstrated the potential of PEG-PLGA nanoparticles for tumor neo-vasculature and tumor cells dual-targeting drug delivery.[42] The ability to focus an external magnetic field within the tumor stroma will not only increase the local concentration of IONPs but also facilitate improved internalization of nanobrick IONPs in endothelial cells. An anticipated result of such focused targeting of the IONPs would be enhanced delivery and potential destruction of the tumor neovasculature. While current anti-angiogenic therapies have been limited in the clinic due to the development of resistance, [43] the targeting of nanobrick IONPs to endothelial cells using shape and magnetic fields would make resistance to these delivery vehicles less probable.

Conclusion

Nanoparticle shape plays an important role in the cellular internalization process. Targeting nanoparticles to endothelial cells can be achieved by modification of shape from a sphere to a brick. Nanobricks exhibited an improved cellar uptake profile compared to nanospheres despite a negative surface charge. The larger overall magnetization of the nanobricks resulted in an enhanced uptake in the presence of an external magnetic field. The preferential uptake of nanobricks in endothelial cells was mediated via caveolae dependent endocytosis. Our results demonstrate that shape modification offers a general approach to achieve targeted delivery.

328 **Table 1: Physico-chemical properties of nanospher and nanobrick IONPs.**

	Nanospheres	Nanobricks
Surface Coating	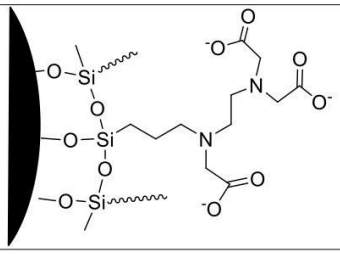	
TEM Size *	8 nm	15 x 10 x 5 nm
Zeta Potential **	-39 ± 3 mV	-45 ± 3 mV
Saturation Magnetization	10 ± 2 A m^2 kg^{-1}	50 ± 5 A m^2 kg^{-1}

329

330 *****IONP core sizes were determined by TEM and reported previously[16, 17]

331 ** surface charges of IONPs were measured in triplicate samples using a Nano-partica SZ-100 series

332 instrument from Horiba. Values represent the mean ± SEM (n=3).

333

Figures

Fig. 1

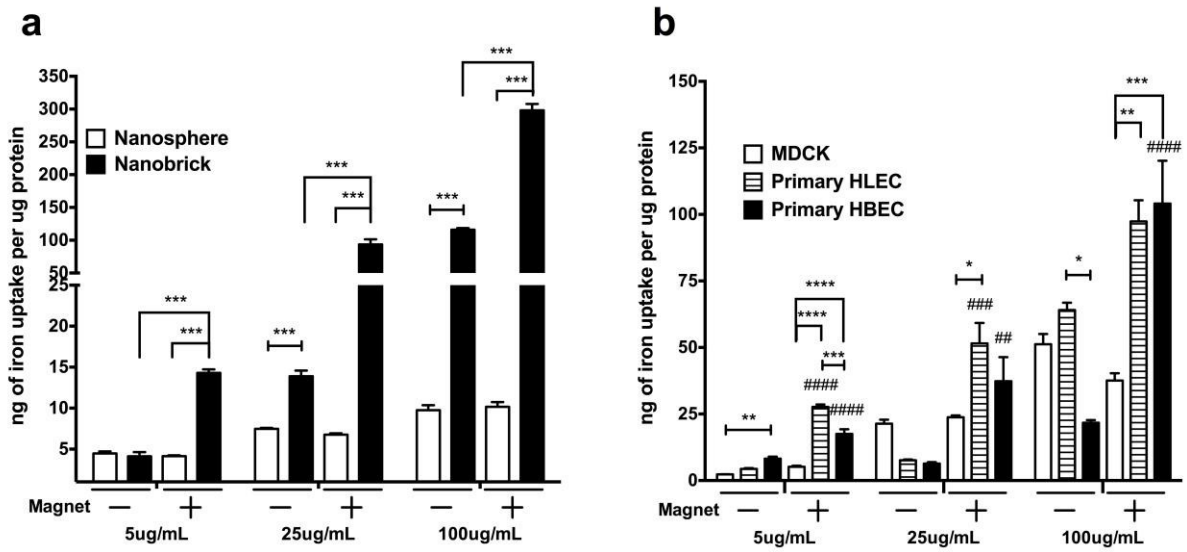

Fig 1 Cellular accumulation of nanobricks and nanospheres in bEnd.3 cells (a). Uptake of nanobricks in MDCK, primary human lung and brain endothelial cells (b). Experiments were performed in the presence and absence of external magnetic field. Values are expressed as the mean ± SEM for three cell monolayers per treatment group. ##, ###, #### indicate $p<0.01$, <0.001, <0.0001 respectively compared to the same treatment group without magnetic filed exposure. *, **, *** and **** indicate $p<0.5$, <0.1, <0.001, and <0.0001.

345 **Fig. 2**

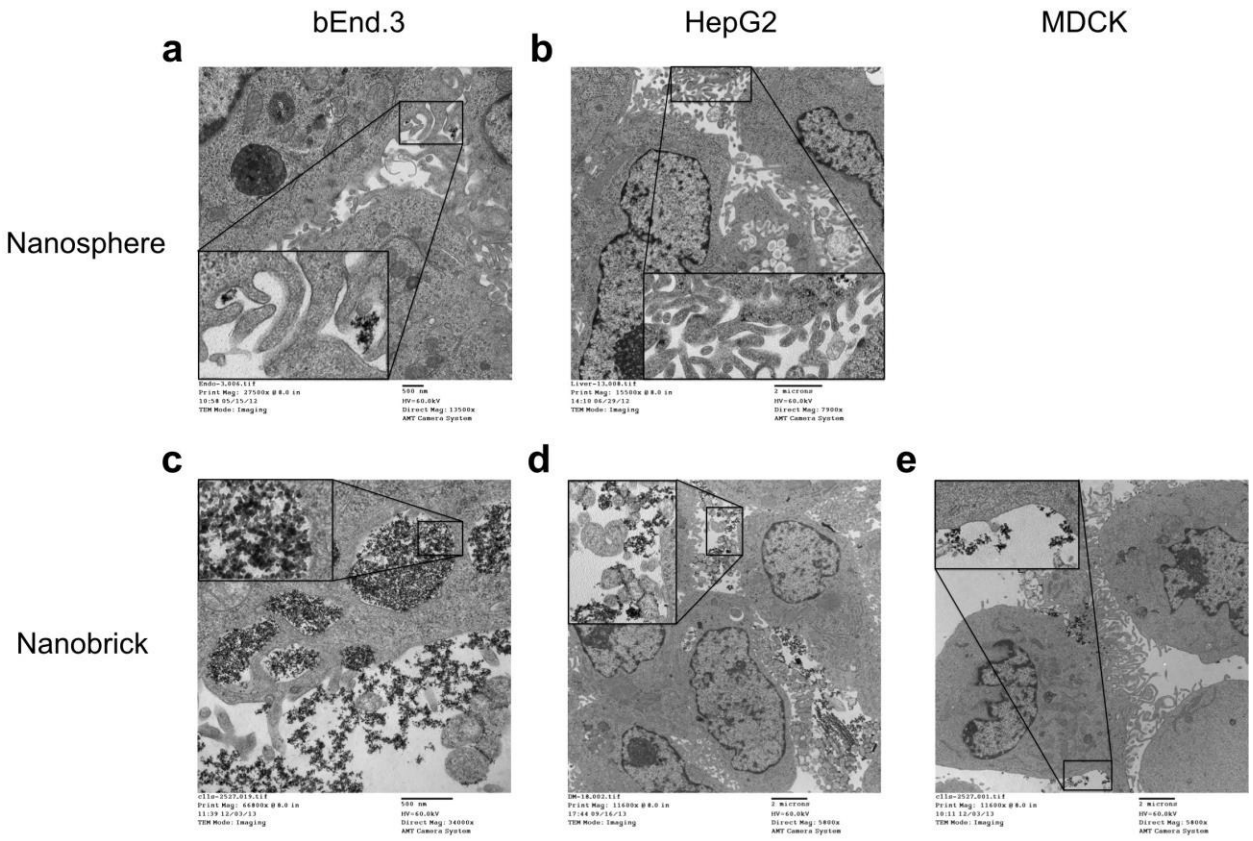

346

347 **Fig 2** Representative TEM images of nanospheres (a, b) and nanobricks (c, d, e) in bEnd.3 (a, c), HepG2

348 (b, d), and MDCK cells (e). The boxed region in each image is magnified 3 times.

349

Fig. 3

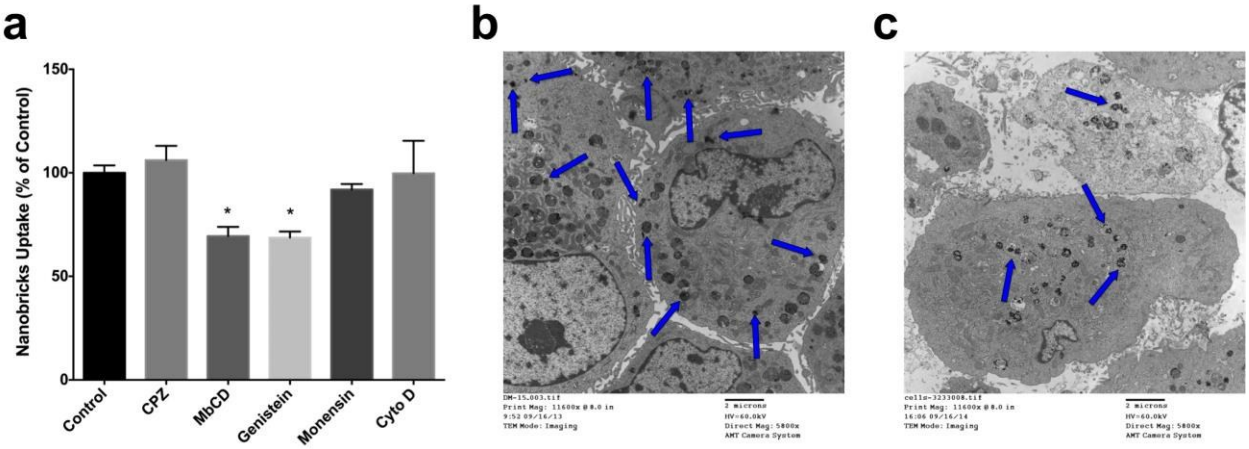

Fig 3 Effect of various endocytosis inhibitors on cellular uptake of nanobricks in bEnd.3 cells. The internalization of nanobricks was significantly decreased by treatment with MβCD and Genistein, inhibitors of caveolae mediated endocytosis. This is confirmed by representative TEM that shows substantially greater internalization of nanobricks under control conditions (b) compared to cells treated with genistein (c). The arrows point to nanoparticles. Values represent the mean ± SEM for three cell monolayers per treatment group; * $p<0.05$ compared to control.

Fig. 4

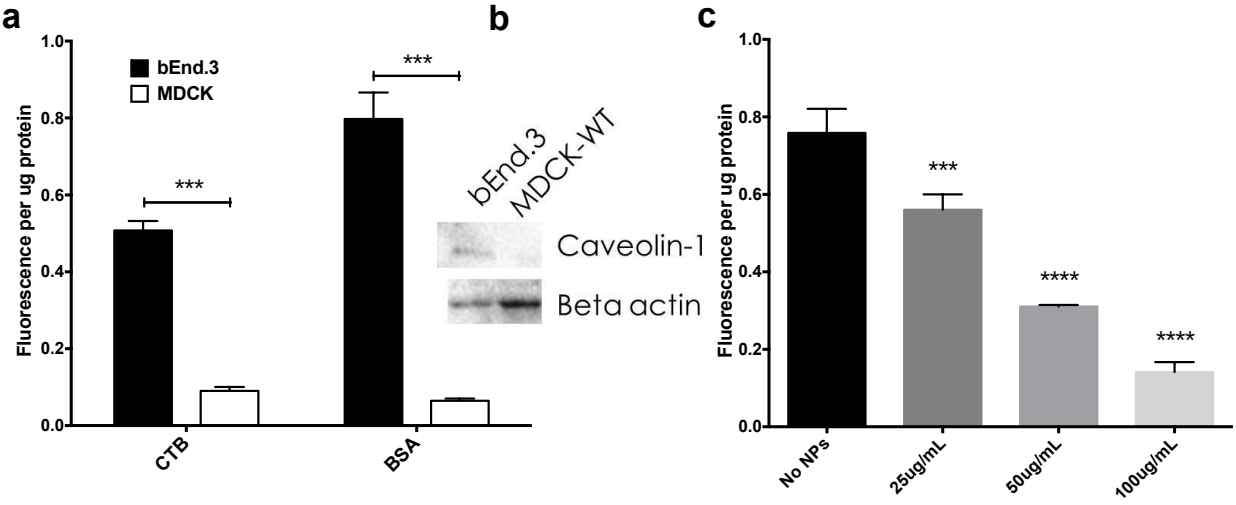

Fig 4 Probing caveolae mediated endocytosis pathway in bEnd.3 and MDCK cells using fluorescently labeled BSA and CTB (markers for caveolae-mediated uptake). Caveolae-mediated pathway is prominent in bEnd.3 cells and significantly lower in MDCK cells (a). Western blot analysis shows higher level of caveolin-1 expression on bEnd.3 cells (b). The ability of nanobricks to inhibit the uptake of fluorescently labeled BSA and CTB in bEnd.3 cells suggests a competitive binding of the nanobricks to the caveolae (c). Values are expressed as the mean ± SEM for three cell monolayers per treatment group. *** indicate $p<0.001$, **** indicate $p<0.0001$.

Acknowledgments

This study was funded by research grants from the Collaborative Health Research Program sponsored by the Canadian Institutes of Health Research and Natural Science and Engineering Research Council of Canada (DWM). This work was also financially supported by the Ohio Third Frontier Ohio Research Scholar Program "Research Cluster on Surfaces in Advanced Materials" (TH). Graduate student fellowship support provided by the Natural Science and Engineering Research Council of Canada (ZS) and the University of Manitoba (YW).

Reference

1. A. K. Silva, N. Luciani, F. Gazeau, K. Aubertin, S. Bonneau, C. Chauvierre, D. Letourneur and C. Wilhelm, *Nanomed.*, 2015, **11**, 645-655.
2. M. E. Mertens, S. Koch, P. Schuster, J. Wehner, Z. Wu, F. Gremse, V. Schulz, L. Rongen, F. Wolf, J. Frese, V. N. Gesche, M. van Zandvoort, P. Mela, S. Jockenhoevel, F. Kiessling and T. Lammers, *Biomaterials*, 2015, **39**, 155-163.
3. J. P. Chen, P. C. Yang, Y. H. Ma and Y. J. Lu, *J. Nanosci. Nanotechnol.*, 2011, **11**, 11089-11094.
4. S. Laurent, A. A. Saei, S. Behzadi, A. Panahifar and M. Mahmoudi, *Expert Opin. Drug Deliv.*, 2014, **11**, 1449-1470.
5. K. Kaaki, K. Herve-Aubert, M. Chiper, A. Shkilnyy, M. Souce, R. Benoit, A. Paillard, P. Dubois, M. L. Saboungi and I. Chourpa, *Langmuir*, 2012, **28**, 1496-1505.
6. Z. Sun, V. Yathindranath, M. Worden, J. A. Thliveris, S. Chu, F. E. Parkinson, T. Hegmann and D. W. Miller, *Int. J. Nanomedicine*, 2013, **8**, 961-970.
7. J. Mai, Y. Huang, C. Mu, G. Zhang, R. Xu, X. Guo, X. Xia, D. E. Volk, G. L. Lokesh, V. Thiviyanathan, D. G. Gorenstein, X. Liu, M. Ferrari and H. Shen, *J. Control. Release*, 2014, **187**, 22-29.
8. E. D. Hood, M. Chorny, C. F. Greineder, S. A. I, R. J. Levy and V. R. Muzykantov, *Biomaterials*, 2014, **35**, 3708-3715.
9. T. Novokhatska, S. Tishkin, V. Dosenko, A. Boldyriev, I. Ivanova, I. Strielkov and A. Soloviev, *Eur. J. Pharmacol.*, 2013, **718**, 401-407.
10. J. Hsu, T. Bhowmick, S. R. Burks, J. P. Kao and S. Muro, *J. Biomed. Nanotechnol.*, 2014, **10**, 345-354.
11. M. Dan, D. B. Cochran, R. A. Yokel and T. D. Dziubla, *PLoS ONE*, 2013, **8**, e81051.
12. H. Yang, F. Zhao, Y. Li, M. Xu, L. Li, C. Wu, H. Miyoshi and Y. Liu, *Int. J. Nanomedicine*, 2013, **8**, 1897-1906.
13. K. Hida, N. Ohga, K. Akiyama, N. Maishi and Y. Hida, *Cancer Sci.*, 2013, **104**, 1391-1395.
14. S. Dasgupta, T. Auth and G. Gompper, *Nano Lett.*, 2014, **14**, 687-693.
15. N. Hao, L. Li and F. Tang, *J. Biomed. Nanotechnol.*, 2014, **10**, 2508-2538.
16. M. Worden, M. A. Bruckman, M.-H. Kim, N. F. Steinmetz, J. M. Kikkawa, C. LaSpina and T. Hegmann, *Journal of Materials Chemistry B*, 2015, **3**, 6877-6884.
17. Z. Sun, M. Worden, Y. Wroczynskyj, V. Yathindranath, J. van Lierop, T. Hegmann and D. W. Miller, *Int. J. Nanomedicine*, 2014, **9**, 3013-3026.
18. J. H. Luft, *The Journal of biophysical and biochemical cytology*, 1961, **9**, 409-414.
19. Z. Sun, V. Yathindranath, M. Worden, J. A. Thliveris, S. Chu, F. E. Parkinson, T. Hegmann and D. W. Miller, *Int. J. Nanomedicine*, 2013, **8**, 961-970.
20. X. M. Zhu, Y. X. Wang, K. C. Leung, S. F. Lee, F. Zhao, D. W. Wang, J. M. Lai, C. Wan, C. H. Cheng and A. T. Ahuja, *Int. J. Nanomedicine*, 2012, **7**, 953-964.
21. Y. Ge, Y. Zhang, J. Xia, M. Ma, S. He, F. Nie and N. Gu, *Colloids Surf. B Biointerfaces*, 2009, **73**, 294-301.
22. A. Villanueva, M. Canete, A. G. Roca, M. Calero, S. Veintemillas-Verdaguer, C. J. Serna, P. Morales Mdel and R. Miranda, *Nanotechnology*, 2009, **20**, 115103.
23. B. Karagoz, J. Yeow, L. Esser, S. M. Prakash, R. P. Kuchel, T. P. Davis and C. Boyer, *Langmuir*, 2014, **30**, 10493-10502.
24. C. de Montferrand, L. Hu, I. Milosevic, V. Russier, D. Bonnin, L. Motte, A. Brioude and Y. Lalatonne, *Acta Biomater.*, 2013, **9**, 6150-6157.
25. W. Xia, H. M. Song, Q. Wei and A. Wei, *Nanoscale*, 2012, **4**, 7143-7148.
26. S. Gil, C. R. Correia and J. F. Mano, *Advanced healthcare materials*, 2015, **4**, 883-891.
27. D. Cheng, X. Li, G. Zhang and H. Shi, *Nanoscale research letters*, 2014, **9**, 195.

28. W. Zhang, M. Kalive, D. G. Capco and Y. Chen, *Nanotechnology*, 2010, **21**, 355103.
29. S. Saito, M. Tsugeno, D. Koto, Y. Mori, Y. Yoshioka, S. Nohara and K. Murase, *Int. J. Nanomedicine*, 2012, **7**, 5415-5421.
30. E. M. Munoz, J. Correa, R. Riguera and E. Fernandez-Megia, *J. Am. Chem. Soc.*, 2013, **135**, 5966-5969.
31. S. Barua, J. W. Yoo, P. Kolhar, A. Wakankar, Y. R. Gokarn and S. Mitragotri, *Proc. Natl. Acad. Sci. U. S. A.*, 2013, **110**, 3270-3275.
32. P. Kolhar, A. C. Anselmo, V. Gupta, K. Pant, B. Prabhakarpandian, E. Ruoslahti and S. Mitragotri, *Proc. Natl. Acad. Sci. U. S. A.*, 2013, **110**, 10753-10758.
33. S. H. Hsu, T. T. Ho and T. C. Tseng, *Biomaterials*, 2012, **33**, 3639-3650.
34. R. G. Parton and K. Simons, *Nat. Rev. Mol. Cell Biol.*, 2007, **8**, 185-194.
35. J. Voigt, J. Christensen and V. P. Shastri, *Proc. Natl. Acad. Sci. U. S. A.*, 2014, **111**, 2942-2947.
36. M. Murata, J. Peranen, R. Schreiner, F. Wieland, T. V. Kurzchalia and K. Simons, *Proceedings of the National Academy of Sciences of the United States of America*, 1995, **92**, 10339-10343.
37. I. M. Adjei, B. Sharma and V. Labhasetwar, *Advances in experimental medicine and biology*, 2014, **811**, 73-91.
38. E. J. Smart, G. A. Graf, M. A. McNiven, W. C. Sessa, J. A. Engelman, P. E. Scherer, T. Okamoto and M. P. Lisanti, *Molecular and cellular biology*, 1999, **19**, 7289-7304.
39. A. El-Sayed and H. Harashima, *Mol. Ther.*, 2013, **21**, 1118-1130.
40. M. Simionescu, D. Popov and A. Sima, *Cell Tissue Res.*, 2009, **335**, 27-40.
41. S. M. Weis and D. A. Cheresh, *Nat. Med.*, 2011, **17**, 1359-1370.
42. G. Gu, Q. Hu, X. Feng, X. Gao, J. Menglin, T. Kang, D. Jiang, Q. Song, H. Chen and J. Chen, *Biomaterials*, 2014, **35**, 8215-8226.
43. J. M. Ebos and R. S. Kerbel, *Nat. Rev. Clin. Oncol.*, 2011, **8**, 210-221.

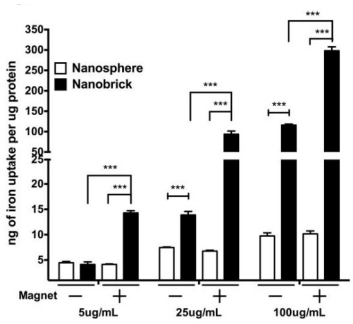

Nonspherical iron oxide core “nanobricks” have enhanced uptake in endothelial cells through caveolae -mediated endocytosis mechanism